1

Suspensions: Basic Principles

Laurier L. Schramm

Petroleum Recovery Institute 100, 3512 33rd Street N.W., Calgary, Alberta
T2L 2A6, Canada

*This chapter introduces the occurrence, properties, and importance
of suspensions in the petroleum industry. The principles of colloid
science are central to an understanding of these suspensions. These
principles may be applied to suspensions in different ways to achieve
quite different results: a stable useful suspension in one application
and the destabilization of an undesirable suspension in another.*

Importance of Suspensions

Suspensions have long been of great practical interest because of
their widespread occurrence in everyday life. Suspensions have impor-
tant properties that may be desirable in a natural or formulated product
or undesirable, such as an unwanted suspension in an industrial process.
Some important kinds of familiar suspensions include those occurring
in foods (batters, puddings, sauces), pharmaceuticals (cough syrups, lax-
atives), household products (inks, paints, "liquid" waxes), and the en-
vironment (suspended lake and river sediments, sewage). Suspensions
are also quite important and widespread in the petroleum industry. In
fact, suspensions may be encountered throughout each of the stages of
petroleum recovery and processing (in reservoirs, drilling fluids, pro-
duction fluids, process plant streams, and tailings ponds) as shown in
the following list:

- migrating fines during secondary and enhanced oil recovery
- dispersions of asphaltenes in crude oils
- produced (well-head) solids in oil recovery
- drilling fluid (mud) suspensions
- well stimulation and fracturing suspensions
- well cementing slurries

- oil sand slurries in the hot water flotation process
- oil sands tailings ponds
- oilfield surface facility sludges

The various suspensions occurring in the petroleum industry may be desirable or undesirable. For example, the classic oilwell drilling fluids (drilling muds) are desirable suspensions. Here, a stable suspension is formulated and used to lubricate the cutting bit and carry cuttings up to the surface. Conversely, certain secondary and enhanced (tertiary) oil recovery processes, if not carefully designed, may cause in situ mobilization or swelling of clays in a reservoir, leading to drastic permeability reduction; in this case, the mobilized clays formed an undesirable suspension.

Suspensions may contain not just solid particles and water but also emulsified oil and even dispersed gas bubbles. In the large Canadian oil sands mining and processing operations, bitumen is disengaged from the sand matrix in suspensions created in large tumblers. The bitumen is then separated from the suspension by a flotation process in which the flotation medium is a suspension of fine particles that also contains emulsified oil (bitumen) and dispersed air bubbles (*see* Chapter 13).

The petroleum industry suspension applications and problems have in common the same basic principles of colloid science that govern the nature, stability, and properties of suspensions. The widespread importance of suspensions in general and scientific interest in their formation, stability, and properties have precipitated a wealth of published literature on the subject. This chapter provides an introduction intended to complement the other chapters on suspensions in this book. A good starting point for further basic information, although focused on clays, is van Olphen's classic book, *An Introduction to Clay Colloid Chemistry* (*1*). There are several other good books on suspensions (*2, 3*), and most good colloid chemistry texts contain introductions to suspensions and some of their properties (*4–8*).

Suspensions as Colloidal Systems

Definition and Classification of Suspensions.   Colloidal particles (or droplets or bubbles) are usually defined as species having at least one dimension between ~1 and 1000 nm (a glossary of frequently encountered particle and suspension terms forms the final chapter of this book; additional information can be found in reference 9). A suspension is a special kind of colloidal dispersion: one in which a solid is dispersed in a continuous liquid phase. The dispersed solid phase is sometimes referred to as the internal (disperse) phase and the continuous phase as the external phase.

Two very different broad types of colloidal dispersions have been distinguished since Graham invented the term "colloid" in 1861 (*10*). Originally, colloids were subdivided into lyophobic and lyophilic colloids (if the dispersion medium is aqueous, then the terms hydrophobic and hydrophilic, respectively, are used). Lyophilic colloids are formed spontaneously when the two phases are brought together, because the dispersion is thermodynamically more stable than the original separated state. The term lyophilic is less frequently used in modern practice because many of the dispersions that were once thought of as lyophilic are now recognized as single-phase systems in which large molecules are dissolved. Lyophobic colloids, which include all petroleum suspensions, are not formed spontaneously on contact of the phases because they are thermodynamically unstable compared with the separated states. These dispersions can be formed with mechanical energy input via some form of agitation, such as that provided by a propeller-style mixer, a colloid mill, or an ultrasound generator. The resulting suspension may well have considerable stability as a metastable dispersion. One may also describe surface properties in terms such as hydrophilic and hydrophobic. For example, smectite clay particles, whose surfaces are strongly hydrophilic, can form quite stable suspensions in water—an example of "hydrophobic dispersion of hydrophilic particles."

Stability.   Lyophobic suspensions are thermodynamically unstable but may be relatively stable in a kinetic sense, so it is crucial that stability be understood in terms of a clearly defined process. A consequence of the small particle size in many suspensions is that quite stable dispersions can be made. That is, the suspended particles may not settle out or float rapidly, and the particles may not aggregate quickly. Some use of the term stability has already been made without definition. In the definition of suspension stability, one considers stability against two different processes: sedimentation (negative creaming) and aggregation. Sedimentation results from a density difference between the two liquid phases. In aggregation two or more particles clump together, touching only at certain points and with virtually no change in total surface area. Aggregation is sometimes referred to as flocculation or coagulation, but for suspensions coagulation and flocculation are frequently taken to represent two different kinds of aggregation. In this case coagulation refers to the formation of compact aggregates in a primary potential energy of interaction minimum, whereas flocculation refers to the formation of a loose network of particles in a secondary potential energy of interaction minimum (*1, 9*). An example can be found in montmorillonite clay suspensions in which coagulation refers to dense aggregates produced by face–face oriented particle associations, and flocculation refers to loose aggregates produced by edge–face or edge–edge oriented particle as-

sociations (1). In aggregation the species retain their identity but lose their kinetic independence because the aggregate moves as a single unit. Kinetic stability can thus have different meanings. A system could be kinetically stable with respect to aggregation but unstable with respect to sedimentation.

Making Suspensions

Colloidal suspensions can be prepared by controlled precipitation of a salt from a supersaturated solution (the aggregation or condensation method), but in the petroleum industry it is more common for colloidal suspensions to be made by the degradation of large particles or aggregates into smaller particles, either dry with subsequent dispersion (size reduction to the order of a few micrometers) or directly in a slurry (size reduction to as small as a few tenths of a micrometer). Whether conducted wet or dry, this is the dispersion method. Factors that aid in the preparation of a suspension include favorable wetting conditions, the absence of strongly bound aggregates, fluid motions in the mixing cell that will submerge the particles, and shear to aid in disaggregation. The dispersion method can be implemented through the application of high shear forces, in a grinding mill or ultrasonic bath, to break up aggregates of particles. It can also be achieved through comminution, where a higher energy input is used to break apart more cohesive aggregates or to literally shatter particles into smaller sizes. To obtain a reasonably stable suspension, some stabilizing (peptizing) electrolyte or surfactant may have to be present as well. Laskowski and Pugh (11) describe and classify the major kinds of inorganic and polymeric dispersing agents used in mineral processing.

For clay minerals the natural processes of weathering and erosion tend to produce small particle sizes so that usually only mild dispersion in simple mixers, blenders, or ultrasonic baths are required. Also for clays, having inherent lattice charge means that when contacted with water, an electric double layer (EDL) is immediately created and no stabilizing (peptizing) electrolyte may be needed in this case. For other solids high energy and physical impact may be required to achieve small particles sizes. In this case grinding in ball or pebble mills may be required, using progressively finer grinding media to achieve finer particle sizes. Figure 1 shows examples of (a) a colloid mill and (b) a ball mill. The principles and operation of several kinds of dispersing equipment are discussed by Ross and Morrison (7). Fallenius (12) presents criteria for suspension for use in scaling turbine and propeller mixers and flotation cells.

Physical Characteristics of Suspensions

Particle Sizes.   Not all suspensions exhibit the opaqueness with which they are usually associated. A suspension can be transparent if

INLET FUNNEL—

COOLANT INLET

HAND WHEEL- ADJUSTING RING

STATOR
ROTOR-

SPILLWAY COVER—

SPILLWAY—

(a)

COOLANT OUTLET

COOLANT INLET

BEARING

Areas show jacketing for heating and cooling with inlets and outlets indicated.

COOLANT OUTLET

(b)
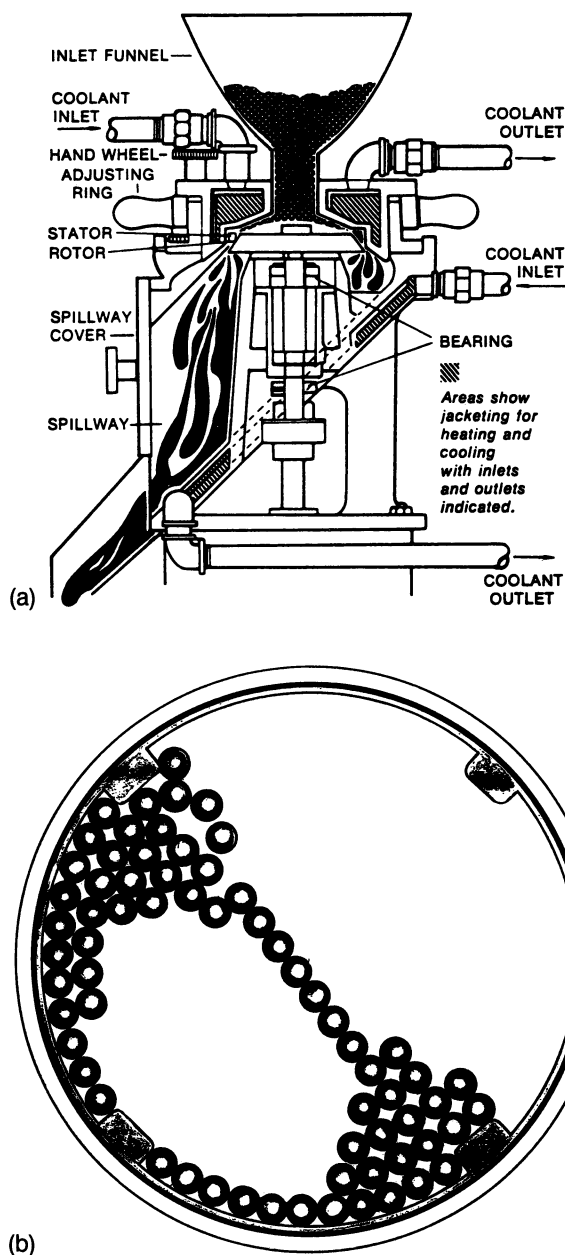
Figure 1. *Examples of (a) a colloid mill and (b) a ball mill used for the preparation of suspensions by the dispersion method. (Figure a courtesy of Premier Mill, Reading, PA. Figure b courtesy of Paul O. Abbé Inc., Little Falls, NJ.)*

particles are sufficiently small compared with the wavelength of the illuminating light. If the particle sizes are 15 nm in diameter, even a 30% suspension will appear to be clear. If the particle sizes are about 1 μm in diameter, a dilute suspension will take on a somewhat milky blue cast. If the particles are very much larger, then the solid phase will become quite distinguishable. Aqueous suspensions may also exhibit different colors due to their scattering of light. A suspension of very fine gold particles (ca. 60 nm) appears red, whereas a suspension of only slightly larger particles (ca. 120 nm) appears blue.

It was stated previously that colloidal particles are between about 10^{-3} and 1 μm in diameter, although in practice, suspension particles are often larger. In fact, suspension particles usually have diameters greater than 0.2 μm and may be larger than 50 μm. Suspension stability is not necessarily a function of particle size, although there may be an optimum size for an individual suspension type. It is very common but generally inappropriate to characterize a suspension in terms of a given particle size because there is inevitably a size distribution. This is usually represented by a histogram of sizes or, if there are sufficient data, a distribution function.

In some suspensions, a particle size distribution that is heavily weighted toward the smaller sizes will represent the most stable suspension. In such cases changes in the size distribution curve with time yield a measure of the stability of the suspensions. The particle size distribution also has an important influence on the viscosity. For electrostatically or sterically interacting particles, suspension viscosity will be higher, for a given mass concentration, when particles are smaller. The viscosity will also tend to be higher when the particle sizes are relatively homogeneous, that is, when the particle size distribution is narrow rather than wide.

If the particle size is large enough and if the suspension is dilute enough, then optical microscopy can be used to determine the size and size distribution. Somewhat smaller particle-size suspensions can be characterized using cryogenic-stage scanning electron microscopy. If the suspension concentration is not too high and the particles are very small, light scattering can yield particle size information. When a beam of light enters a suspension, some light is absorbed, some is scattered, and some is transmitted. Many dilute fine suspensions show a noticeable turbidity given by

$$I_t/I_0 = \exp(-\tau l) \tag{1}$$

where I_t is the intensity of the transmitted beam, I_0 the intensity of the incident beam, τ is the turbidity, and l is the length of the path through the sample.

From Rayleigh theory, the intensity of light scattered from each particle depends largely on its size and shape and on the difference in refractive index between the particle and the medium. For a suspension, each spherical particle scatters light at an intensity I_d at a distance x from the particle, according to the following relationship:

$$I_d/I_0 \propto r^6/x^2\lambda^4 \tag{2}$$

where λ is the wavelength of the light and r is the particle radius. Because the scattering intensity is proportional to $1/\lambda^4$, blue light ($\lambda = 450$ nm) is scattered much more than red light ($\lambda = 650$ nm). With incident white light, a dilute suspension of 0.1–1 μm-sized particles will, therefore, tend to appear blue when viewed at right angles to the incident light beam. If the particles are less than 50 nm or so, the suspension will appear to be transparent.

Concentrated suspensions are more difficult to study by optical methods. A detailed description of other approaches to characterizing particles is given in Chapter 2.

Ultramicroscopy.   When a testtube containing a dilute suspension of very small particles is held up to the light, it will appear to have a blue color due to Rayleigh scattering. Because this happens for particles so small they would be invisible under the light microscope (less than about a micrometer), this phenomenon suggests a way to observe particles that would otherwise be invisible. In the darkfield microscope, or ultramicroscope, the light scattered by small particles is viewed against a dark background. This method is used to observe the electrophoretic motions of colloidal particles, to be discussed later.

Rayleigh theory gives another relation from which particle sizes can be obtained. In the limit as the particle concentration goes to zero,

$$Kc/R_{90} = 1/M \tag{3}$$

where R_{90} is $R(\theta)$ for a scattering angle of 90°, M is the molar mass of particles, c is the concentration of particles, and $K = (2\pi^2n_0^2/N_A\lambda^4)(dn/dc)^2$; n_0 is refractive index of the solvent and N_A is Avogadro's number. The value dn/dc is measured with a differential refractometer. Once M is obtained, a knowledge of the particle density allows calculation of the average equivalent spherical diameter. This approach can be used to obtain the size of very small particles, ca. 20 nm diameter. For larger particles the theory is more involved.

Conductivity.   Of the numerous equations proposed (*12*) to describe the conductivity of dispersions (κ), one is cited here for illustration. The Bruggeman equation gives

$$(\kappa - \kappa_D)(\kappa_C/\kappa)^{1/3} = (1 - \phi)(\kappa_C - \kappa_D) \qquad (4)$$

where ϕ is the dispersed phase volume fraction, κ_D is the conductivity of the dispersed phase, and κ_C is that of the continuous phase. If $\kappa_C \gg \kappa_D$, then $(\kappa/\kappa_C) = (1 - \phi)^{3/2}$. Further discussion of suspension conductivity and some practical examples for suspensions flowing in pipelines are given in Chapter 4.

The fact that the presence of solid particles can influence bulk conductivity forms the basis for a family of particle-size measuring techniques known as sensing-zone techniques. A well-known implementation of this is in the Coulter counter. A dilute suspension is allowed to flow through a small aperture (sensing zone) between two chambers. The conductivity (or resistance) between the chambers changes when a particle passes through the aperture. The degree of change is related to the particle volume, hence size.

The sensing-zone techniques are not limited to conductivity but may involve the measurement of capacitance. Figure 2 shows an example of the use of capacitance monitoring in a vertical sedimentation vessel. In this case (14) the effective suspension permittivity was measured and used to estimate the solids concentration (expressed in terms of volume fraction).

Rheology. The rheological properties of a suspension are very important. High viscosity may be the reason that a suspension is troublesome, a resistance to flow that must be dealt with, or a desirable property for which a suspension is formulated. The simplest description applies to Newtonian behavior in laminar flow. The coefficient of viscosity, η, is given in terms of the shear stress, τ, and shear rate, $\dot{\gamma}$, by

$$\tau = \eta\dot{\gamma} \qquad (5)$$

where η has units of mPa·s. Many colloidal dispersions, including concentrated suspensions, do not obey the Newtonian equation. For non-Newtonian fluids the coefficient of viscosity is not a constant but is itself a function of the shear rate; thus

$$\tau = \eta(\dot{\gamma})\dot{\gamma} \qquad (6)$$

It is common for industrial pumping and processing equipment to use shear rates that fall in the intermediate shear regime from about 10 to 1000 s^{-1} as illustrated in Table I. A convenient way to summarize the flow properties of fluids is by plotting flow curves of shear stress versus shear rate (τ vs $\dot{\gamma}$). These curves can be categorized into several rheological classifications (Figure 3). Suspensions are frequently pseudoplastic: as shear rate increases viscosity decreases. This is also termed
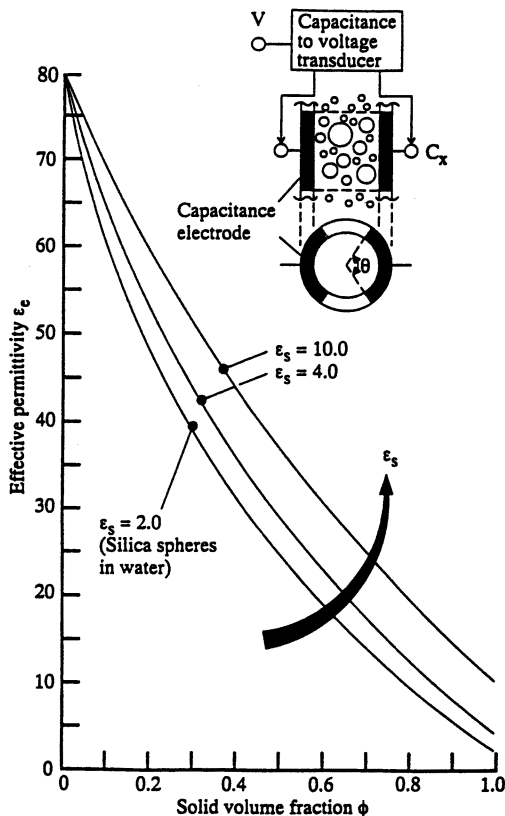
Figure 2.   Capacitance monitoring in a sedimentation vessel (inset) and the relation between effective suspension permittivity ϵ_e and solids concentration in the suspension for spherical particles of permittivity ϵ_s in liquid of permittivity ϵ_L. (Reproduced from reference 14. Copyright 1992 Butterworth-Heinemann.)

Table I.   Approximate Values of Shear Rate Appropriate to Various Processes

Process	Approximate Shear Rate (s^{-1})	Ref.
Very slow stirring	0.01–0.1	52
Reservoir flow in oil recovery	1–5	53
Mixing	10–100	52
Pumping	100–1000	52
Coating	10,000	52
Oilwell drilling fluid at the bit nozzle	10,000–100,000	54
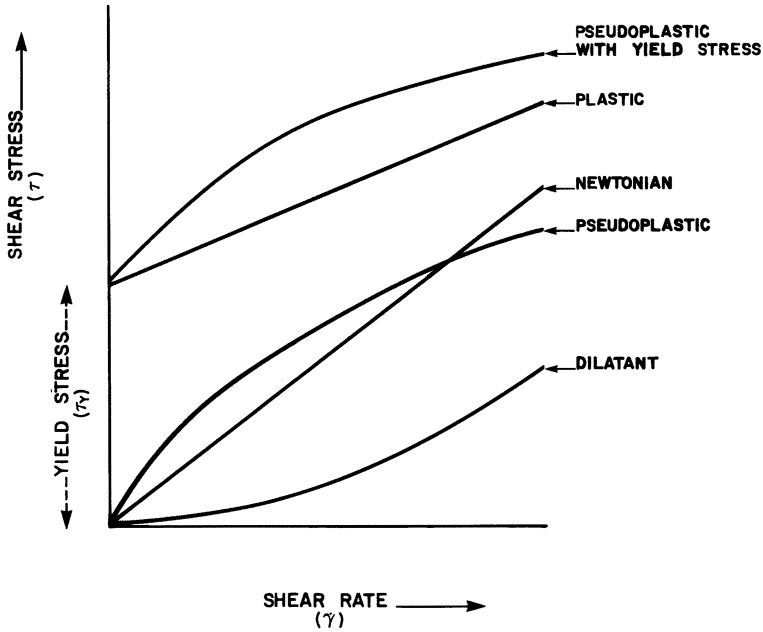
Figure 3.   Illustration of the characteristic fluid types and their corresponding flow curves.

shear-thinning. A suspension may also exhibit a yield stress, that is, the shear rate (flow) remains zero until a threshold shear stress is reached, referred to as the yield stress (τ_Y), and then pseudoplastic or Newtonian flow begins. Some descriptions appropriate to different yield stresses are given in Table II. Pseudoplastic flow, which is time-dependent, is termed thixotropic, that is, at a constant applied shear rate viscosity

Table II.   Some Descriptions Appropriate to Different Yield Stresses

Yield Stress (Pa/s)	Description
<10	Easy to pour.
10–30	Thick, pours easily.
	Use conventional liquid designs.
30–40	Thick, hard to pour, forms peaks.
	Difficult to make flow under pump suction.
40–100	Flows poorly; will cleave to walls under gravity.
	Need to push into pump suction.
>100	Can build with it; will cleave to top of jar.
	Requires positive flow pump.

SOURCE: Adapted from reference 52.

decreases and in a flow curve hysteresis occurs. It is also not unusual for suspensions that are pseudoplastic at low to moderate solids concentrations to become dilatant (shear thickening) at high solids concentrations. In this case there is also a critical shear rate for the onset of shear thickening. Several other rheological classifications are covered in the glossary of this book.

Whorlow (*15*) and others (*16, 17*) described very useful experimental techniques. Very often, measurements are made with a suspension sample placed in the annulus between two concentric cylinders. The shear stress is calculated from the measured torque required to maintain a given rotational velocity of one cylinder with respect to the other. Knowing the geometry, the effective shear rate can be calculated from the rotational velocity. Less useful are the various kinds of simplified measuring devices found in many industrial plants and even in their technical support laboratories. Such devices may not be capable of determining shear stresses for known shear rates or may not be capable of operation at shear rates that are appropriate to the process under consideration. Instruments that are capable of absolute viscosity measurements provide much more useful information.

In an attempt to conduct rheological measurements on suspensions, a number of changes may occur in the sample chamber, making the measurements irreproducible and not representative of the original suspension. Prevalent among these changes is the sedimentation, or even centrifugal segregation, of solids, causing a nonuniform distribution within the measuring chamber. In the extreme sedimentation can cause complete removal of solids from the region in which measurements are made.

It is frequently desirable to be able to describe suspension viscosity in terms of the viscosity of the liquid continuous phase (η_0) and the amount of suspended material. A very large number of equations have been advanced for estimating suspension (or emulsion, etc.) viscosities. Most of these are empirical extensions of Einstein's equation for a dilute suspension of spheres:

$$\eta = \eta_0(1 + 2.5\phi) \tag{7}$$

where η_0 is the medium viscosity and ϕ is the dispersed phase volume fraction ($\phi < 1$). Examples of two empirical equations are the Oliver–Ward equation for spheres (*9*):

$$\eta = \eta_0(1 + a\phi + a^2\phi^2 + a^3\phi^3 + \cdots) \tag{8}$$

where a is an empirical constant, and the Thomas equation for suspensions:

$$\eta = \eta_0(1 + 2.5\phi + 10.5\phi^2 + 0.00273 \exp[16.6\phi]) \tag{9}$$

These equations apply to Newtonian behavior, or at least the Newtonian region of a flow curve, and they usually require that the particles not be too large and have no strong electrostatic interactions.

Other modifications have been made for application to suspensions of anisometric (unsymmetric) particles such as clays. In this case the intrinsic viscosity $[\eta]$, given by

$$[\eta] = \lim_{\phi \to 0} \lim_{\dot{\gamma} \to 0} (\eta/\eta_0 - 1)/\phi \qquad (10)$$

which is 2.5 for a dilute suspension of uncharged spheres, takes on a value that is different and more difficult to predict value. A useful such modification to Einstein's equation for dilute suspensions of anisometric particles is given by the Simha Equation, which is approximately

$$\eta = \eta_0(1 + a\phi/1.47b) \qquad (11)$$

where a is the major particle dimension and b the minor particle dimension.

A more detailed treatment of these kinds of relationships is given in Chapter 3.

Suspensions can show varying rheological, or viscosity, behaviors. Sometimes these properties are due to stabilizing agents in the suspension. However, typically particle–particle interactions are sufficient to cause the suspension viscosity to increase because of electrostatic interactions or simply particle "crowding."

Stability of Suspensions

Most suspensions are not thermodynamically stable. Rather, they possess some degree of kinetic stability, and it is important to distinguish the degree and the time scale of change. In this discussion of colloid stability, we explore the reasons why colloidal suspensions can have different degrees of kinetic stability and how these are influenced, and can therefore be modified, by solution and surface properties. Encounters between particles in a suspension can occur frequently due to Brownian motion, sedimentation, stirring or a combination of them. The stability of the dispersion depends on how the particles interact when this happens. The main cause of repulsive forces is the electrostatic repulsion between like charged objects. The main attractive forces are the van der Waals forces between objects.

Electrostatic Charges.   Most substances acquire a surface electric charge when brought into contact with a polar medium such as water. For suspensions, the origin of the charge can be due to

- ionization or surface hydrolysis, as when carboxyl and/or amino functionalities dissociate when proteins are put into water (pH dependent)

- ion adsorption, as when surfactant ions adsorb onto a solid surface

- ion dissolution, as when Ag^+ and I^- dissolve unequally from their crystal lattice when AgI is placed in water (Ag^+ and I^- are potential determining ions)

- ion diffusion, as when a dry clay particle is placed in water and the counterions diffuse out to form an EDL

The surface charge influences the distribution of nearby ions in the polar medium. Ions of opposite charge (counterions) are attracted to the surface, whereas those of like charge (coions) are repelled. An EDL, which is diffuse because of mixing caused by thermal motion, is thus formed.

Electric Double Layer.   The EDL consists of the charged surface and a neutralizing excess of counterions over coions, distributed near the surface (Figure 4). The EDL can be viewed as being composed of two layers: an inner layer, which may include adsorbed ions, and a diffuse layer, in which ions are distributed according to the influence of electrical forces and thermal motion. Gouy and Chapman proposed a simple quantitative model for the diffuse double layer assuming, among other things, an infinite, flat, uniformly charged surface and point charge ions. Taking the surface potential to be $\psi°$, the potential ψ at a distance x from the surface is approximately

$$\psi = \psi° \exp(-\kappa x) \qquad (12)$$

The surface charge density is given as $\sigma° = \epsilon \kappa \psi°$, where ϵ is the permittivity; thus, $\psi°$ depends on surface charge density and the solution ionic composition (through κ). $1/\kappa$ is called the double layer thickness and for water at 25 °C is given by

$$\kappa = 3.288 \sqrt{I} \qquad (13)$$

where κ is given in nm^{-1}, I is the ionic strength, given by $I = (1/2) \Sigma_i c_i z_i^2$. For 1–1 electrolyte, $1/\kappa$ is about 1 nm in 10^{-1} M ionic strength solution and about 10 nm in 10^{-3} M ionic strength solution.

In fact, an inner layer exists because ions are not really point charges, and an ion can only approach a surface to the extent allowed by its hydration sphere. The Stern model incorporates a layer of specifically adsorbed ions bounded by a plane, called the Stern plane (Figure 5). In
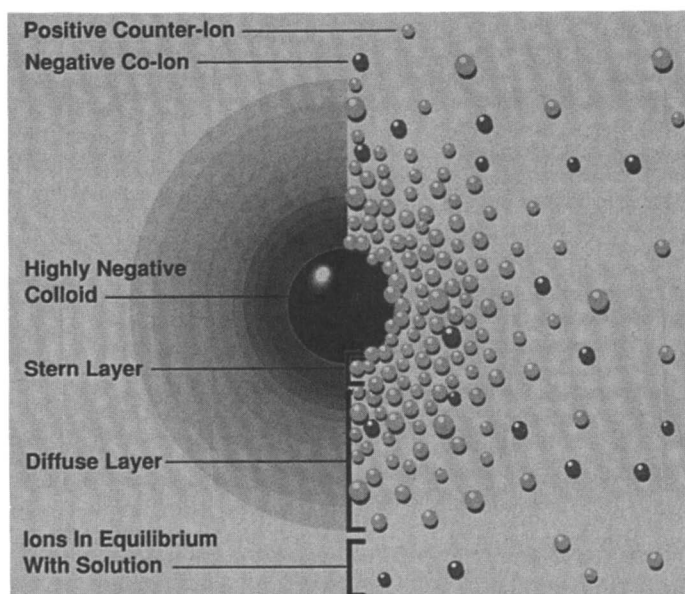
Figure 4.   Simplified illustrations of the electrical double layer around a negatively charged colloidal suspension particle. The left view shows the change in charge density around the drop. The right view shows the distribution of ions around the charged drop. (Courtesy L. A. Ravina, Zeta-Meter, Inc., Staunton, VA.)

this case the potential changes from $\psi°$ at the surface, to $\psi(\delta)$ at the Stern plane, to $\psi = 0$ in bulk solution.

Electrokinetic Phenomena.   Electrokinetic motion occurs when the mobile part of the EDL is sheared away from the inner layer (charged surface). There are four types of electrokinetic measurements, electrophoresis, electroosmosis, streaming potential, and sedimentation potential, of which the first finds the most use in industrial practice. Good descriptions of practical experimental techniques in electrophoresis and their limitations can be found in references 18–20.

In electrophoresis an electric field is applied to a sample, causing charged particles or particles plus any attached material or liquid, to move toward the oppositely charged electrode. Thus, the results can only be interpreted in terms of charge density (σ) or potential (ψ) at the plane of shear. The latter is also known as the zeta potential. Because the exact location of the shear plane is generally not known, the zeta potential is usually taken to be approximately equal to the potential at the Stern plane (Figure 5):

$$\zeta \approx \psi(\delta). \tag{14}$$
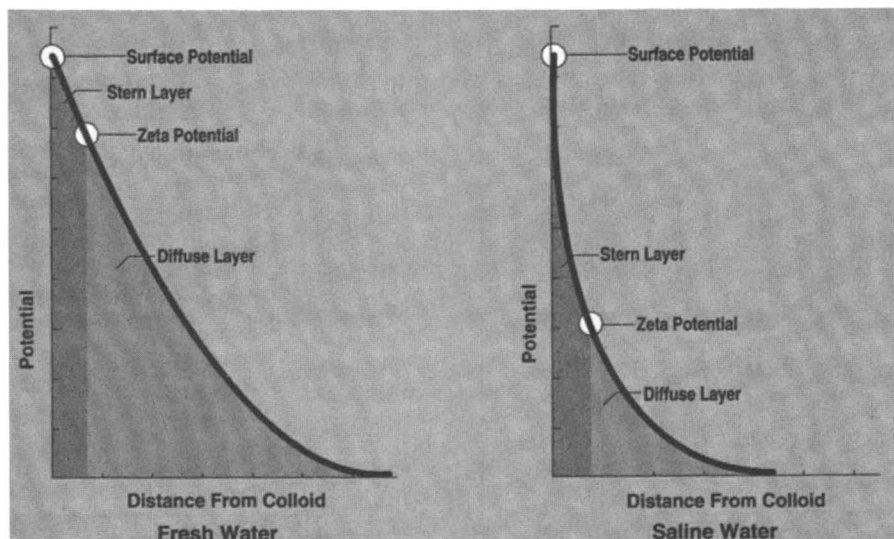
Figure 5.   Simplified illustration of the surface and zeta potentials for a charged suspension drop dispersed in high (saline water) and low (fresh water) electrolyte concentration aqueous solutions. (Courtesy L. A. Ravina, Zeta-Meter, Inc., Staunton, VA.)

In microelectrophoresis the dispersed particles are viewed under a microscope and their electrophoretic velocity is measured at a location in the sample cell where the electric field gradient is known. This must be done at carefully selected planes within the cell because the cell walls become charged as well, causing electroosmotic flow of the bulk liquid inside the cell.

The electrophoretic mobility, μ_E, is defined as the electrophoretic velocity divided by the electric field gradient at the location where the velocity was measured. It remains then to relate the electrophoretic mobility to the zeta potential (ζ). Two simple relations can be used to calculate zeta potentials in limiting cases:

Hückel Theory.   For particles of small radius, a, with "thick" EDLs, meaning that $\kappa a < 1$, it is assumed that Stokes law applies and the electrical force is equated to the frictional resistance of the particle, $\mu_E = \zeta\epsilon/(1.5\ \eta)$.

Smoluchowski Theory.   For large particles with "thin" EDLs, meaning particles for which $\kappa a > 100$, $\mu_E = \zeta\epsilon/\eta$. With these relations, zeta potentials can be calculated for many practical systems. Note that within each set of limiting conditions the electrophoretic mobility is

independent of particle size and shape as long as the zeta potential is constant. For intermediate values of κa, the Henry equation and many other equations are available in the literature (*18, 19, 21*).

Repulsive Forces. In the simplest example of colloid stability, suspension particles would be stabilized entirely by the repulsive forces created when two charged surfaces approach each other and their EDLs overlap. The repulsive potential energy V_R for spherical particles is given approximately as

$$V_R = (B\epsilon k^2 T^2 a\gamma^2/z^2) \exp[-\kappa x] \tag{15}$$

where the spheres have radius a and are separated by distance x. In Figures 6 and 7, H and d have the same meaning as x. B is a constant (3.93×10^{39} A^{-2} s^{-2}), z is the counterion charge number, and

$$\gamma = (\exp[ze\psi(\delta)/2kT] - 1)/(\exp[ze\psi(\delta)/2kT] + 1) \tag{16}$$

In practice the situation may be more complicated. If particle surfaces are covered by long chain molecules (physically or chemically bonded to the surface), then steric repulsion between particles may be significant. This repulsion is due to an osmotic effect caused by the high concentration of chains that are forced to overlap when particles closely approach and also due to the volume restriction, or entropy decrease, that occurs when the chains lose possible conformations because of overlapping.

Dispersion Forces. van der Waals postulated that neutral molecules exert forces of attraction on each other that are caused by electrical interactions between dipoles. The attraction results from the orientation of dipoles due to any of (1) Keesom forces between permanent dipoles, (2) Debye induction forces between dipoles and induced dipoles, or (3) London–van der Waals forces between induced dipoles and induced dipoles. Except for quite polar materials, the London–van der Waals dispersion forces are the most significant of the three. For molecules the force varies inversely with the sixth power of the intermolecular distance.

For dispersed particles (or droplets, etc.) the dispersion forces can be approximated by adding up the attractions between all interparticle pairs of molecules. When added this way, the dispersion force between two particles decays less rapidly as a function of separation distance than is the case for individual molecules. For two spheres of radius a in vacuum, separated by a small distance x, the attractive potential energy V_A can be approximated by

$$V_A = -Aa/12x \tag{17}$$

for $x < 10$–20 nm and $x << a$. The constant A is known as the Hamaker constant and depends on the density and polarizability of atoms in the particles. Typically, $10^{-20} J < A < 10^{-19} J$, or $2.5kT < A < 25kT$ at room temperature (*21*). When the particles are in a medium other than vacuum, the attraction is reduced. This can be accounted for by using an effective Hamaker constant

$$A = (\sqrt{A_2} - \sqrt{A_1})^2 \qquad (18)$$

where the subscripts denote the medium (1) and particles (2).

The effective Hamaker constant equation shows that the attraction between particles is weakest when the particles and medium are most chemically similar ($A_1 \approx A_2$). The Hamaker constants are usually not well known and must be approximated.

DLVO Theory.   Derjaguin and Landau (*23*) and, independently, Verwey and Overbeek (*24*) developed a quantitative theory for the stability of lyophobic colloids, now known as the DLVO theory. It was developed in an attempt to account for the observation that colloids coagulate quickly at high electrolyte concentrations, slowly at low concentrations, and with a very narrow electrolyte concentration range over which the transition from one to the other occurs. The latter defines the critical coagulation concentration (CCC). The DLVO theory accounts for the energy changes that take place when two particles approach each other and involves estimating the potential energy of attraction (dispersion forces) versus interparticle distance and the potential energy of repulsion (electrostatic forces) versus distance. These estimates, V_A and V_R, are then added together to yield the total potential interaction energy V. There are deviations from DLVO theory that appear at very small separation distances: the first is a short-range repulsive force that occurs in aqueous systems and may be due to an influence of the particle surfaces on hydrogen-bonding in nearby water molecules (*25*) and the second is a strong short-range repulsive force due to atomic electron cloud overlap, called Born repulsion. The DLVO theory has been developed for several special cases, including the interaction between two spheres, and refinements are constantly being made.

V_R decreases exponentially with increasing separation distance and has a range about equal to κ^{-1}, while V_A decreases inversely with increasing separation distance. Figure 6 shows a single attractive potential energy curve and two different repulsive potential energy curves, representing two very different levels of electrolyte concentration. The figure shows the total potential interaction energy curves that result in each case. It can be seen that either the attractive van der Waals forces or the repulsive electric double layer forces can predominate at different interparticle distances.

Where there is a positive potential energy maximum, a dispersion should be stable if $V >> kT$, that is, if the energy is large compared to the thermal energy of the particles ($15kT$ is considered unsurmountable). In this case colliding particles should rebound without contact and the suspension should be stable to aggregation. If, on the other hand, the potential energy maximum is not very great, $V \approx kT$, then slow aggregation should occur. The height of the energy barrier depends on the surface potential, $\psi(\delta)$ and on the range of the repulsive forces, κ^{-1}. Figure 6 shows that a secondary potential energy minimum can occur at larger interparticle distances. If this is reasonably deep compared with kT, then a loose easily reversible aggregation should occur. Figure 7a illustrates the effects of altering the height of the potential energy maximum. Here computer simulations were conducted (26) for the interaction between two spherical particles based on DLVO theory. As particles approach each other and pass through the secondary minimum, they experience a small (case I) or a large (case II) energy barrier that has to be surmounted to reach the primary potential energy well. In this case the energy barrier was adjusted by reducing the concentration of indifferent electrolyte for case II. The effects on the proportions of primary particles versus aggregated particles are shown in Figure 7b. A smaller energy barrier to be surmounted results in a much higher proportion of aggregated versus primary particles.
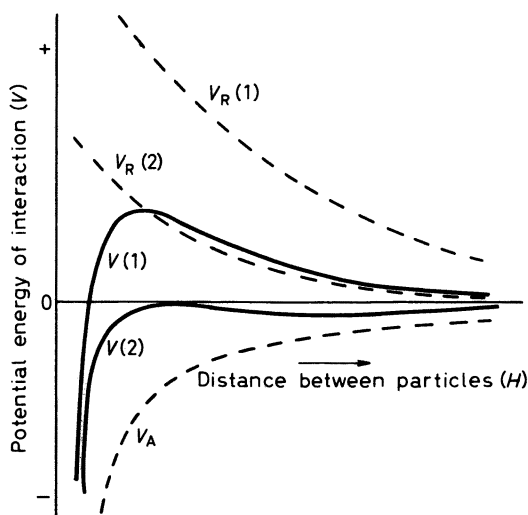
Figure 6.   The effect of different repulsive potential energy curves V_R *(1) and* V_R *(2) on the total potential energy of interaction curves* V *(1) and* V *(2), for a given attractive potential energy curve. (Reproduced with permission from reference 4. Copyright 1981 Butterworth-Heinemann.)*
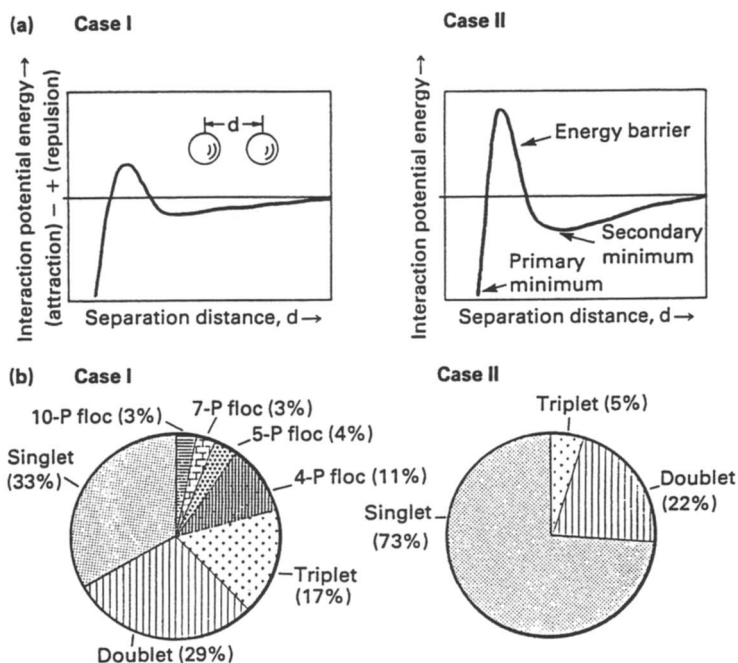
Figure 7. *Interaction energy curves (a) for two spherical particles in the presence of two different concentrations of indifferent electrolyte. Also shown (b) are the aggregation statistics, in terms of the percentages of primary particles versus aggregates, obtained from computer simulations for each case. (Reproduced with permission from reference 26. Copyright 1992 Society of Chemical Industry.)*

Practical Guidelines. It is apparent that the DLVO calculations can become quite involved, requiring considerable knowledge about the systems of interest. Also, there are some problems. For example, the prevailing assessment of the validity of the theory is changing as more becomes known about the influence of additional forces, such as those due to surface hydration. In addition, there is now considerable effort being devoted to the possibility of directly determining the forces between colloidal particles, which for the present can only be inferred. For a recent review on this topic and the use of the surface force apparatus, *see* reference 25. The DLVO theory nevertheless forms a very useful starting point in attempting to understand complex colloidal systems such as petroleum suspensions. There are empirical "rules of thumb" that can be used to give a first estimate of the degree of colloidal stability that a system is likely to have if the zeta potentials of the particles are known.

Many types of colloids tend to adopt a negative surface charge when dispersed in aqueous solutions that have ionic concentrations and pH

typical of natural waters. For such systems one rule of thumb stems from observations that the colloidal particles are quite stable when the zeta potential is about -30 mV or more negative and quite unstable because of agglomeration when the zeta potential is between $+5$ and -5 mV. An expanded set of guidelines, developed for particle suspensions, is given by Riddick (20). Such criteria are frequently used to determine optimal dosages of polyvalent metal electrolytes, such as alum, used to effect coagulation in treatment plants.

Water treatment, whether for drinking water or for disposal of industrial wastes, inevitably involves removal of suspended solids (often referred to as turbidity) usually silt, clay, and organic matter. The charge on the solids is sufficiently negative to yield a stable dispersion that settles slowly and is difficult to filter. The solution to this problem is to reduce the zeta potential to values that permit rapid coagulation, increasing both sedimentation and filterability. A first step toward coagulating the suspension might be to add aluminum sulfate (alum), from which the trivalent aluminum ions will have a powerful effect on the zeta potential (remembering the Schulze–Hardy rule). Figure 8 shows an example of this effect. In practice, however, the alum required to reduce the zeta potential to below about -10 mV or so reduces the solution pH too much. Unreacted alum becomes carried to other parts of the plant and forms undesirable precipitates. As shown in Figure 9, a second step can be introduced then, in which a cationic polyelectrolyte is added to reduce the zeta potential to a near zero value (slightly positive in the example in Figure 9) but without changing the pH. As a final step, a high molecular weight anionic polymer may be added (molecular weight 500,000 to 1,000,000 or more) whose molecules can bridge between agglomerates, yielding very large rapid settling flocs.

Schulze–Hardy Rule.   The transition from stable dispersion to aggregation usually occurs over a fairly small range of electrolyte concentration. This makes it possible to determine aggregation concentrations, often referred to as critical coagulation concentrations (CCC). The Schulze–Hardy rule summarizes the general tendency of the CCC to vary inversely with the sixth power of the counterion charge number (for indifferent electrolyte).

A prediction from DLVO theory can be made by deriving the conditions under which $V = 0$ and $dV/dx = 0$. The result is

$$CCC = (9.75B^2\epsilon^3k^5T^5\gamma^4)/(e^2N_AA^2z^6) \qquad (19)$$

showing that for high potentials ($\gamma \to 1$), the CCC varies inversely with z^6. As an illustration, suppose that for a hypothetical suspension equation 19 predicts a CCC of 1.18 M in solutions of sodium
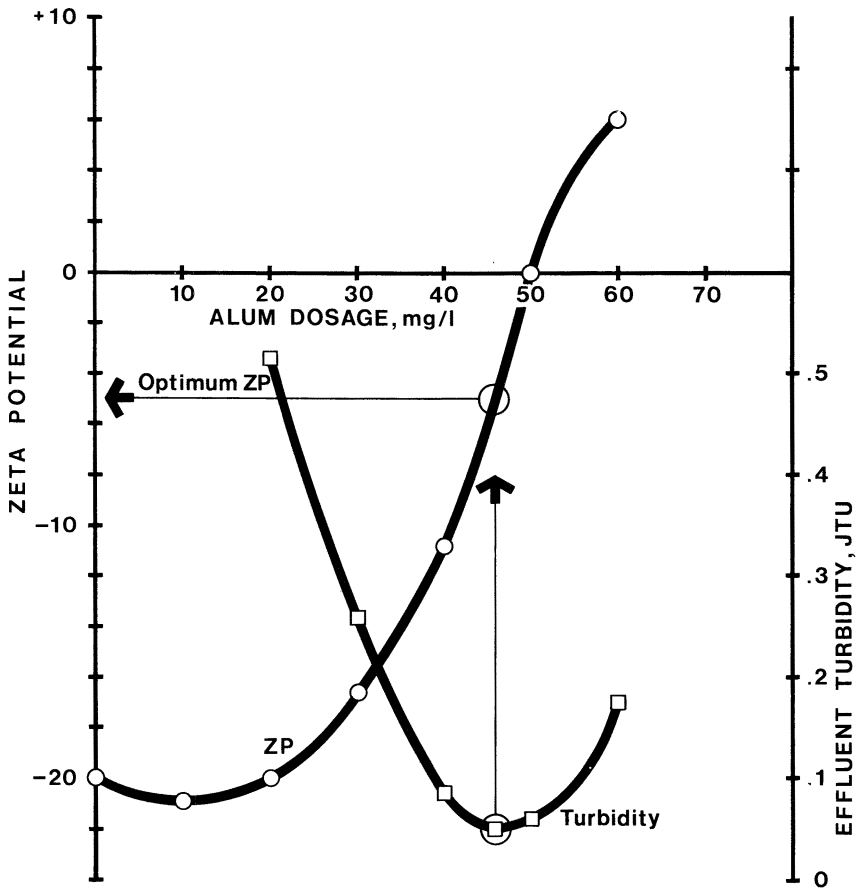
Figure 8. Illustration of the effects of alum treatment on particle Zeta potentials and turbidity levels in water treatment. (Courtesy L. A. Ravina, Zeta-Meter, Inc., Staunton, VA.)

chloride. The CCC in polyvalent metal chlorides would then decrease as follows:

Dissolved Salt	z	CCC (mol/L)
NaCl	1	1.18
CaCl$_2$	2	0.018
AlCl$_3$	3	0.0016

Protective Agents, Steric Stabilization, and Flocculation. The transitions from stable dispersion to aggregation just described in terms of the CCC and the Schulze–Hardy rule apply best to suspensions
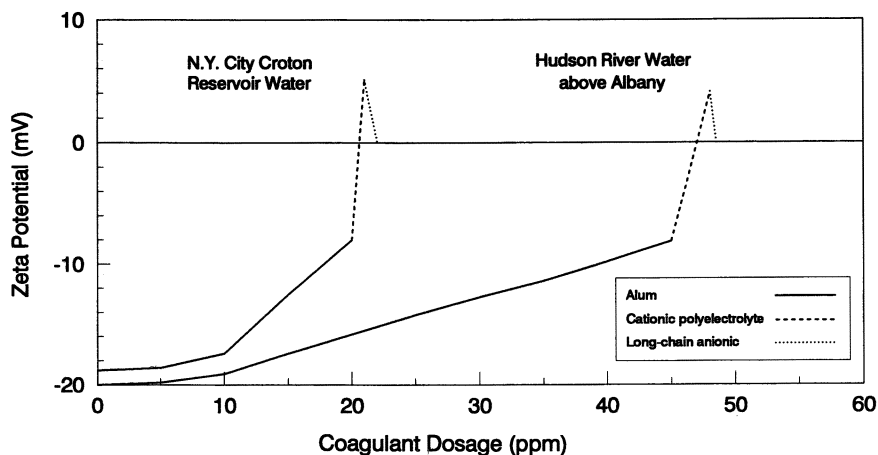
Figure 9.   Illustration of zeta potentials and coagulation of solids in New York city water treatment through sequential additions of aluminum sulfate (alum), cationic polyelectrolyte, and anionic polymer. (Reproduced with permission from reference 50. Copyright 1982 Zeta-Meter, Inc.)

in which the particles have only one kind of charge. But clay particles can carry positive and negative charges at the same time, on different parts of the particle. The clay minerals are composed (*1, 27*) of sheets of tetrahedrally coordinated silica and sheets of octahedrally coordinated alumina or magnesia. These sheets occur stacked upon one another, forming platelike layers or particles. When dispersed in aqueous solutions of near neutral to alkaline pH, the particles carry a net negative charge, largely due to isomorphic substitution of cations of lower charge for cations of higher charge within the lattice (e.g., Al^{+3} for Si^{+4} in tetrahedral sheets and Fe^{+2} or Mg^{+2} for Al^{+3} in the octahedral sheet; Figure 10). Meanwhile, the edges of clay particles may carry a positive charge in near neutral to acid pH solution because of protonation of various atoms exposed at the edges.

   This heterogeneous charge distribution leads to a number of kinds of particle interaction orientations in clay suspensions as shown in Figure 11. Three basic modes are possible: face–face (FF), edge–face (EF), and edge–edge (EE). The different modes can be combined in different ways depending on the clay mineralogy (montmorillonite has higher negative charge density than kaolinite, for which the positive edge charging can be more significant), solution pH (directly determining the contributions from edge charging), solution ionic composition, and solution ionic strength (both of which affect aggregation overall and also the number of plates per tactoid in aggregates; *see* references 28 and 29).

   The stability of a suspension can be enhanced (protection) or reduced (sensitization) by the addition of material that adsorbs onto particle sur-
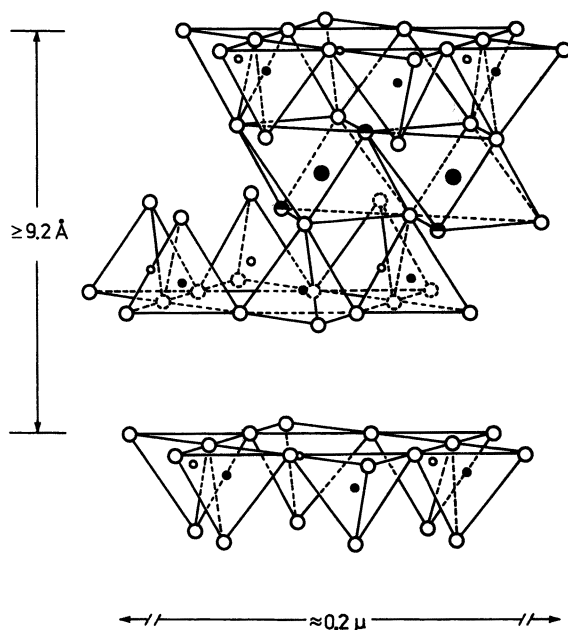
Figure 10. *Illustration of the basic structure of smectite clay minerals. Lattice positions are assigned as silicon (• and ○); aluminum, magnesium, or iron (●); oxygen (○); and hydroxyl (◖). (Reproduced with permission from reference 27. Copyright 1968 McGraw Hill.)*
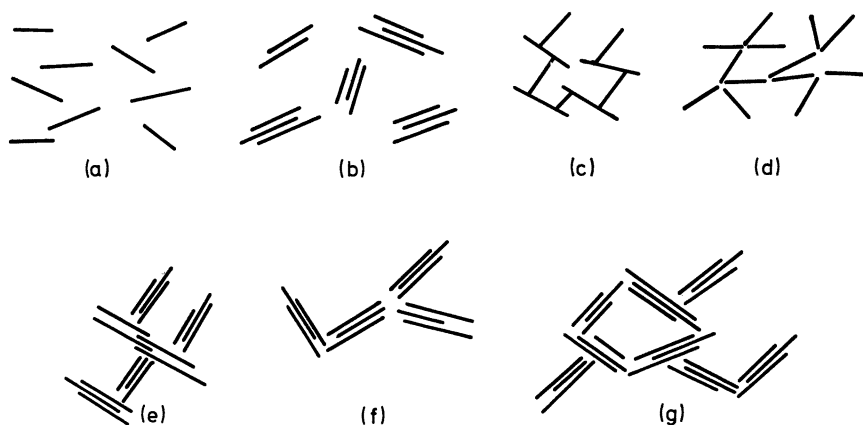
Figure 11. *Some possible modes of clay particle association: (a) dispersed, (b) coagulated into tactoids, (c and d) flocculated primary particles, and (e–g) coagulated and flocculated particles. Face–face mode is shown as b, edge–face mode is c, edge–edge mode is d, and others are mixtures of these. (Reproduced with permission from reference 51. Copyright 1980 Laurier L. Schramm.)*

faces (Figure 12). Protective agents can act in several ways. They can increase double layer repulsion if they have ionizable groups. The adsorbed layers can lower the effective Hamaker constant. An adsorbed film may necessitate desorption before particles can approach closely enough for van der Waals forces to cause attraction. If the adsorbed material extends out significantly from the particle surface, then an entropy decrease can accompany particle approach (steric stabilization). Oilfield suspensions of particles in oil may be stabilized by the presence of an adsorbed film formed from the asphaltene and resin fractions of the crude oil.

In steric stabilization adsorbed polymer molecules must extend outward from the particle surface yet be strongly enough attached to the surface that they remain adsorbed in the presence of applied shear. An example is a system of particles containing terminally anchored block copolymer chains having a hydrophobic portion of the molecule that is very strongly adsorbed on the particle surfaces and a hydrophilic part
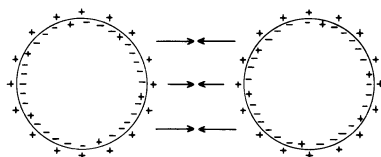
METHOD 1: Mutual repulsion due to high Zeta Potential
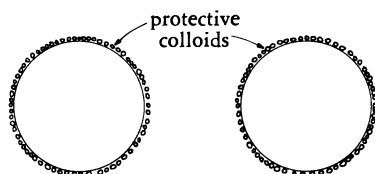
METHOD 2: Adsorption of a small lyophilic colloid on a
larger electronegative colloid
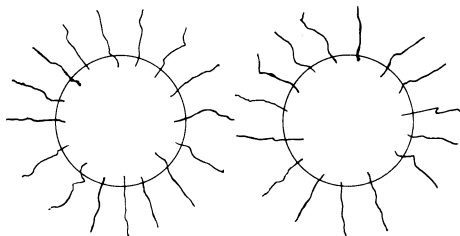
METHOD 3: Steric hindrance due to adsorption of an
oriented nonionic polyelectrolyte

Figure 12.   Illustration of three means of promoting colloid stability. (Courtesy of Zeta-Meter Inc., Staunton, VA.)

of the molecule that extends outward from the particle surfaces. The size of the adsorbed molecule determines the extent of the long-range repulsive force between particles and also causes the primary minimum to disappear (Figure 13). Curve A shows an example for electrostatically stabilized particles. Curves B–D show examples for sterically stabilized particles in three different polymer stabilizer and solvent systems. As the figure shows, sterically stabilized particles are either stably dispersed or reversibly aggregated (flocculated) in a secondary minimum. By changing the nature of the medium, such a suspension can be adjusted back and forth between the stable and flocculated conditions. It is also possible to have particles stabilized by both electrostatic and steric stabilization; these are said to be electrosterically stabilized.

Flocculation of particles may be achieved through the addition to a suspension of high molecular mass (millions of g/mol) synthetic or natural polymers. These molecules act as bridging agents by adsorbing onto more than one particle at a time with a significant portion of the polymer chain still remaining in the aqueous phase. The bridging action causes the formation of porous flocs. The formation of such flocs has a dramatic effect on sedimentation rates, sediment volumes, and on the ease of filtration. Effective flocculation may occur over a narrow range of polymer concentration because too little polymer will not permit floc formation whereas too much polymer adsorption will eliminate the fraction of free particle surface needed for the bridging action (i.e., the polymer molecules will adsorb onto single particles in preference to bridging several particles). The nature of the flocculation is quite dependent on experimental conditions such as the nature and degree of agitation that may be present.

The process of stabilizing a suspension by reversing the processes of aggregation (coagulation and/or flocculation) is known as peptization, or deflocculation. This can be accomplished by attacking the mechanisms that cause, or caused, aggregation in the first place. For example, in the case of clay suspensions, some of the well-known peptizing agents act
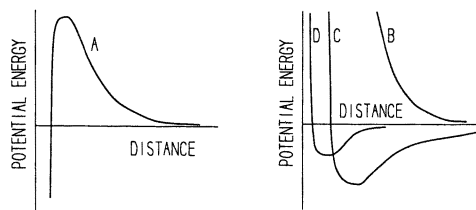
Figure 13. Potential energy diagrams for (A) electrostatically stabilized particles and (B–D) sterically stabilized particles with different degrees of steric stabilization. (Reproduced with permission from reference 7. Copyright 1988 Wiley.)

via the adsorption of anionic species at clay particle edges in sufficient quantity to reverse the charge. This weakens or eliminates the forces, causing EF and EE clay-plate associations. Given the small specific surface area of clay particle edges, it can be seen that this could be accomplished by very small additions of peptizing chemical. Figure 14 shows the effect of adding a peptizing agent to a clay suspension on the clay salt-flocculation value in a flocculation diagram. The point where all three curves intersect the vertical axis shows the flocculation value of the suspension to an indifferent salt (sodium chloride) alone. Curve 1 shows how addition of peptizing agent (sodium polymetaphosphate) increases the salt flocculation value. The curve shows that overdosing (overtreatment) is possible and that at very high additions the peptizer acts as a flocculating agent even without the original sodium chloride addition. Curve 2 shows the additive effect of using an agent that is similar to the original salt (in this case potassium chloride). Curve 3 illustrates the situation in which the agent added makes the suspension more susceptible to flocculation by the original salt (synergism).

Kinetics.   Thus far we have mostly been concerned with an understanding of the direction in which reactions will proceed. However, from an engineering point of view, it is just as important to know the rates at which such reactions will proceed. Two principal factors determine the rate of aggregation of particles in a suspension: the frequency of particle encounters and the probability that the thermal energy of the particles is sufficient to overcome the potential energy barrier to
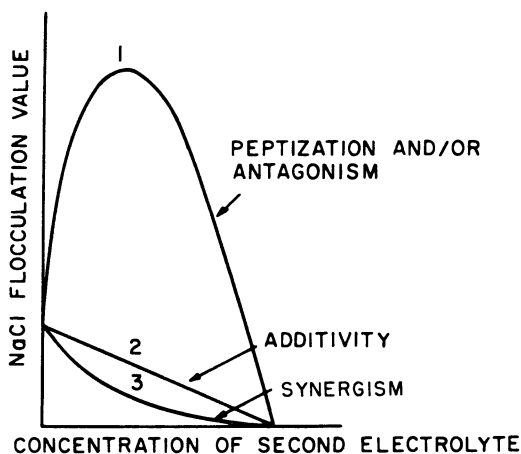
Figure 14.   Effects of a mixture of sodium chloride and different potential peptizing agents on the NaCl flocculation value (suspension stability). (Reproduced with permission from reference 1. Copyright 1977 Wiley.)

aggregation. The rate of aggregation can be given as $-(dn/dt) = k_2 n^2$, where n is the number of particles per unit volume at time t and k_2 is the rate constant. For $n = n_0$ at $t = 0$, $1/n = k_2 t + 1/n_0$. During the process of aggregation, k_2 may not remain constant.

If the energy barrier to aggregation is removed (e.g., by adding excess electrolyte), then aggregation is diffusion controlled—only Brownian motion of independent particles is present. For a monodisperse suspension of spheres, Smoluchowski developed an equation for this rapid coagulation:

$$n = n_0/(1 + 8\pi Dan_0 t) \tag{20}$$

where a is the radius and the diffusion coefficient $D = kT/(6\pi\eta a)$. Now $k_2^0 = 4kT/(3\eta)$, where k_2^0 is the rate constant for diffusion controlled aggregation.

When there is an energy barrier to aggregation, only a fraction $1/W$ of encounters lead to attachment. W is the stability ratio $W = k_2^0/k_2$. Using W allows one to account for "slow coagulation" (hindered) times. In this case, the interaction energy and hydrodynamic viscous drag forces must be considered (*4*). For example, Alince and Van de Ven (*30*) studied the rate of destabilization of clay particles by pH adjustment and by cationic polyethylenimine addition. They found that the stability ratio could be correlated with the electrophoretic mobility of the clay particles and that the maximum rate of destabilization corresponded to conditions for which the electric charge on the clay particles or aggregates was nearly zero.

Finally, particles can also be brought into interaction distances by stirring or sedimentation where the relative motions of two adjacent regions of fluid, each carrying particles, can cause particle encounters. Coagulation due to such influence is called orthokinetic coagulation as distinguished from the Brownian-induced perikinetic coagulation. The theory for orthokinetic coagulation is much more complicated than that for perikinetic and is not dealt with here. It should be remembered, however, that shear can also cause dispersion if the energy introduced allows the interaction energy barrier to be overcome. (For more information on aggregation kinetics *see* references 31–33).

Electrostatic Properties in Nonaqueous Media. Although suspensions most commonly comprise particles dispersed in aqueous media, the petroleum industry contains many examples of particles dispersed in nonaqueous media. Examples include precipitated asphaltenes in oil (*see* Chapter 8) and mineral solids dispersed in diluted froth in oil sands processing (*see* Chapter 13). Particles can be electrostatically stabilized in nonaqueous media, although the charging mechanism is different (*7, 34*). In a recent review Morrison (*34*) emphasized that many models are

available for the behavior of electrical charges in nonaqueous media but few are universally accepted. The particles may acquire their charge by adsorption of ions or through the dissociation of ions from their surfaces. In one model of nonaqueous electrolyte solutions, the ions are considered to be held in large structures such as micelles that prevent their being neutralized. The electric field, its concentration dependence, and the electrical conductivity then are determined by the size, structure, and motions of these micelles.

In the petroleum industry flammable vapors are often present so both fire and explosion hazards exist. The conductivity of petroleum fluids is low, which allows the buildup of large potential gradients. The interaction of impurities in the petroleum fluids with pipe and tank walls apparently allows the generation of electrical charges (there is also a role for emulsified water droplets). The flow of the fluid in a tank or pipe allows the separation of charges and can cause sufficient charging for an electrostatic discharge, which in turn can cause an explosion. According to Morrison (34), appropriate safety precautions include keeping all containers and pipes electrically connected, increasing the electrical conductivity of the petroleum fluid by adding nonaqueous electrolytes, and keeping the environment free of oxygen.

The role of electrostatic repulsion in the stability of suspensions of particles in nonaqueous media is not yet clear. To apply the DLVO theory, one must know the electrical potential at the surface, the Hamaker constant, and the ionic strength to be used for the nonaqueous medium; these are difficult to estimate. The ionic strength will be low so the EDL will be thick, the electric potential will vary slowly with separation distance, and so will the net electric potential as the double layers overlap. For this reason the repulsion between particles can be expected to be weak. A summary of work on the applicability or lack of applicability of DLVO theory to nonaqueous media has been given by Morrison (34).

Sedimentation

Particles in a suspension will have some tendency to settle, possibly according to Stokes' law. In general, an uncharged spherical particle in a fluid will sediment out if its density is greater than that of the fluid. The driving force is that of gravity; the resisting force is viscous and is approximately proportional to the particle velocity. After a short period of time, the particle reaches terminal (constant) velocity dx/dt when the two forces are matched. Thus,

$$dx/dt = (2a^2(\rho_2 - \rho_1)g)/(9\eta) \tag{21}$$

where a is the particle radius, ρ_2 is the particle density, ρ_1 is the external fluid density, g is the gravitational constant, and η is the bulk viscosity. If the particle has a lower density than the external phase, then it rises instead (negative sedimentation, flotation, or creaming). In the cases of electrostatically interacting particles or particles with surfactant or polymeric stabilizing agents at the interface, the particles will interact, contrary to the assumption of this theory. Thus, Stokes' law will not strictly apply and may underestimate or even overestimate the real terminal velocity.

For dense particles in a suspension, the individual settling (kinetic) units may be primary particles, coagulated aggregates, or flocculated aggregates (flocs). If a given mass of solid is dispersed in liquid and placed in a sedimentation column (Figure 15), then the sedimentation volume, or specific sedimentation volume, can be determined as a function of time. A qualitative result is that the settling behaviors of the primary (deflocculated), coagulated, and flocculated particles are different and lead to different specific sedimentation volume–time curves, as shown in Figures 16 and 17. It can be seen that the packing densities in the particles translate into the same order of packing densities in the sediment, although given sufficient time these structures will change and become increasingly dense. A very simple settling test sometimes used in industrial plants is to establish a standard procedure for agitating a sample of suspension in a given size jar, allowing the suspension to stand, and measuring the time required for the particles to settle out. A time scale appropriate to the process under consideration is then set. For example, fast-settling suspensions might be those that settle out completely within 10 min. After the settling test, the jar can be agitated again to check the ease of resuspension.

| (a) | (b) | (c) | (d) |
| Pipette method | Hydrometer method | Oden's balance | Wiegner's tube |
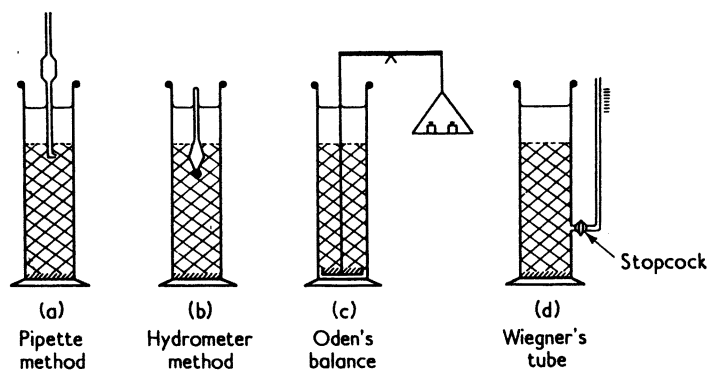
Figure 15.   Sedimentation columns used for the determination of sedimentation rates and particle size distributions in suspensions. (Reproduced with permission from reference 52. Copyright 1959 Karol J. Mysels.)

(a)
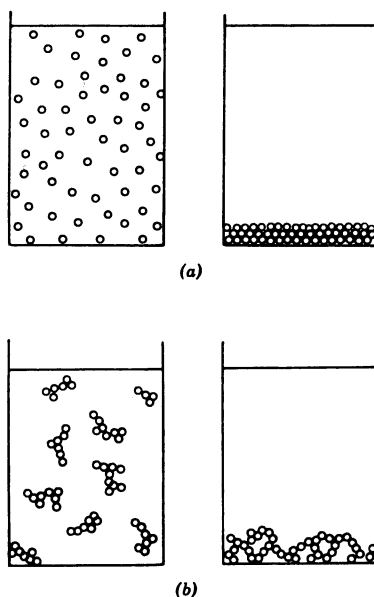
Figure 16. Sedimentation of (a) primary particles leading to a close-packed sediment and (b) flocculated particles leading to a loose-packed voluminous sediment. (Reproduced with permission from reference 1. Copyright 1977 Wiley.)

(b)

A quantitative result is illustrated by the following example taken from Hiemenz (5). By using the Oden balance of Figure 15, one can measure the total mass W (in mass% units) of sedimenting clay particles that reach the balance pan at various times t. This is shown in Figure 18a. Here, W is made up of particles large enough to have fallen the full length of the column (w) and also a fraction of those that have are only able to fall part of the height of the column but that nevertheless
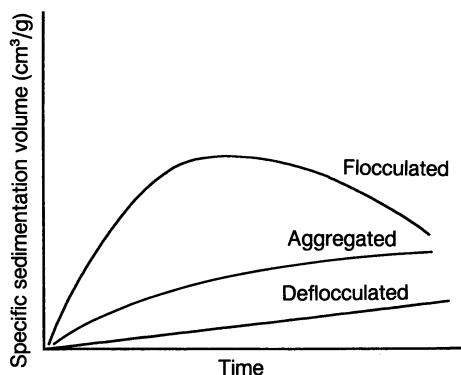
Figure 17. Specific sedimentation volume versus settling time curves for deflocculated (primary) particles, coagulated aggregates, and flocculated aggregates of particles. (Reproduced with permission from reference 7. Copyright 1988 Wiley.)
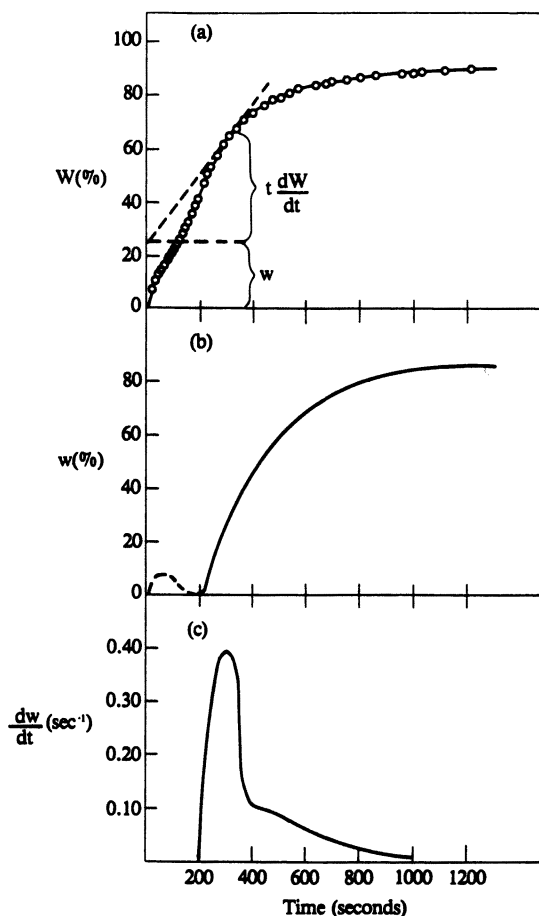
Figure 18.   Example of the sedimentation of particles in a clay suspension, monitored using an Oden balance, showing (a) the measured cumulative mass of particles collected versus time; (b) a graphical derivative of the first curve, with respect to time, showing the cumulative mass of oversize particles; and (c) a graphical second derivative of the first curve, with respect to time, showing the frequency by mass of particles. (Reproduced with permission from reference 5. Copyright 1986 Marcel Dekker.)

reach the balance pan ($t\,dW/dt$). Here, dW/dt is the slope of the curve in Figure 18a at time t and measures the rate of accumulation of particles smaller than the cutoff size at that time. The intercepts of the tangents dW/dt drawn for various times t yield the values of w for each time. Figure 18b shows a plot of w versus t, the accumulated mass of particles greater than the cutoff size at any time. This is an integrated size distribution curve for particles greater than the cutoff size. Figure 18c

shows a graphical differentiation of Figure 18b and is the particle size distribution curve. Although this is not a very accurate method, it shows that in this example the distribution has a significant peak corresponding to a clay particle size that settles in 300 s. By introducing an assumption about particle shape, one can apply a model and calculate particle sizes. Assuming that the particles are spheres and that Stokes' law applies the calculated peak, particle size in this example turns out to be about 24 μm diameter (using $\Delta\rho = 2.17$ g/mL and height 20 cm).

Enhanced Gravity Sedimentation.   It can be seen from Stokes' law that sedimentation will occur faster when there is a larger density difference and when the particles are larger. The rate of separation can be enhanced by replacing the gravitational driving force by a centrifugal field. Centrifugal force, like gravity, is proportional to the mass, but the proportionality constant is not g but $\omega^2 x$, where ω is the angular velocity ($=2\pi \times$ revolutions per s) and x is the distance of the particle from the axis of rotation. The driving force for sedimentation becomes $(\rho_2 - \rho_1) \omega^2 x$. Because $\omega^2 x$ is substituted for g, one speaks of multiples of g, or g's, in a centrifuge. The centrifugal acceleration in a centrifuge is not really a constant throughout the system but varies with x. Because the actual distance from top to bottom of a sedimenting column is usually small compared with the distance from the center of revolution, the average acceleration is used. The terminal velocity then becomes

$$dx/dt = (2a^2(\rho_2 - \rho_1)\omega^2 x)/(9\eta) \tag{22}$$

As an illustration, consider the problem of removing solids and water droplets from deaerated bituminous froth produced from the oil sands hot water flotation process (*see* Chapter 13 and reference 35). This is a nonaqueous suspension from which the particles and water droplets must be removed before upgrading and refining. At process temperature (80 °C) the suspension viscosity is similar to that of bitumen alone, but the density, because of the dispersed solids, is higher. Taking $\eta = 500$ mPa·s (35), $\rho_1 = 1.04$ g/mL and $\rho_2 = 2.50$ g/mL, the rate of settling of 10 μm diameter solid particles under gravitational force will be very slow:

$$dx/dt = (2a^2(\rho_2 - \rho_1)g)/(9\eta)$$

$$dx/dt = 1.59 \times 10^{-5} \text{ cm/s}$$

$$dx/dt = 1.37 \text{ cm/d}$$

In a commercial oil sands plant, a centrifuge process is used to speed up the separation. The continuous centrifuges can operate at 2500 g,

the particles having to travel 9 cm to reach the product stream. With the centrifugal force added, the particle velocity would become

$$(dx/dt)' = (2a^2(\rho_2 - \rho_1)\omega^2 x)/(9\eta)$$

$$(dx/dt)' = 2500(dx/dt)$$

$$(dx/dt)' = 3.98 \times 10^{-2} \text{ cm/s}$$

This is 2500 times faster than with gravity alone, but the residence time in the centrifuge would have to be about 4 min. If to speed up the separation naphtha is added to the level of 25 vol%, it will lower the viscosity to about 4.5 mPa·s (36) and lower the density of the continuous phase to 0.88 g/mL. The particle velocity now becomes $(dx/dt)'' = 4.9$ cm/s, which yields a satisfactory residence time of about 2 s. In this particular example the centrifuges also have to separate out emulsified water droplets for which the calculations are analogous but the results are somewhat different (37).

   In general, sedimentation will occur more slowly the greater the electrical charge on the particles and the higher the suspension viscosity. Although a distinct process, sedimentation does promote coagulation by increasing the particle crowding and hence the probability of particle–particle collisions.

Energetics of the Interfaces

In simple two-phase colloidal systems, a thin intermediate region or boundary, known as the interface, lies between the dispersed and dispersing phases. Interfacial properties are very important because dispersed colloidal particles have a large interfacial area. Even a modest interfacial energy per unit area can become a considerable total interfacial energy. There is more surface energy in a two-phase system when the dispersed phase is highly subdivided than there is when it is coarsely subdivided. This is why colloidal dispersions have unique properties and why they so often can only be prepared by applying high shearing forces to break down larger particles, droplets, or bubbles.

   The ratio of surface or interfacial area to mass of material is termed the specific surface area of a substance, A_{sp}. Consider the specific surface area of two 1-g samples of silica spheres for which in sample 1 the spheres are 1 mm in diameter and in sample 2 they are 1 μm in diameter. The total mass of each is the same (density 2 g/mL), but they do not have the same amount of surface area. For n spheres of density ρ and radius R we have

$$A_{sp} = [(\# \text{ particles})(\text{area/particle})]/[(\# \text{ particles})(\text{mass/particle})]$$

$$A_{sp} = [n4\pi R^2]/[n(4\backslash 3)\pi R^3 \rho]$$

$$A_{sp} = 3/(\rho R) \tag{23}$$

Sample 1, containing the 1-mm diameter spheres, has a specific surface area of $A_{sp} = 0.0030$ m^2/g, whereas sample 2, containing the 1-μm diameter spheres, has a specific surface area of $A_{sp} = 3.0$ m^2/g. The sample of smaller particles has 1000 times more surface area. Schramm (37) provides an example of the emulsification of one barrel (159 L) of oil into water by repeatedly subdividing a large droplet into droplets until the initial radius of $r = 33.6$ cm becomes 0.64 μm. This represents an interfacial area increase of over five orders of magnitude.

Consider the molecules in a liquid. The attractive van der Waals forces between molecules are felt equally by all molecules except those in the interfacial region. This pulls the latter molecules toward the interior of the liquid. The interface thus has a tendency to contract spontaneously. This is the reason particles of liquid and bubbles of gas tend to adopt a spherical shape: it reduces the surface free energy, or surface tension. For the interface between a solid and a liquid, a similar situation applies, and an imbalance of intermolecular forces will still occur, except that the interface may not be able to curve. The surface free energy has units of mJ/m^2 (1 mJ/m^2 = 1 erg/cm^2) showing that area expansion requires energy. Surface free energies are usually described in terms of contracting forces acting parallel to the surface or interface. Surface tension ($\gamma°$), or interfacial tension (γ), is the force per unit length around a surface, or the free energy required to create new surface area. Thus, the units of surface and interfacial tension are mN/m (1 mN/m = 1 dyne/cm). These units for surface and interfacial tension are numerically equal to the surface free energy.

There are many methods available for the measurement of surface and interfacial tensions. Most of these techniques and their limitations are discussed in several good reviews (38–40). While numerous other properties have been investigated many times for aqueous colloidal suspensions, their surface and interfacial tensions have not received much attention. In fact, it is quite common in industrial practice, when dealing with such systems, to remove the solids and measure and report surface and interfacial tensions on a solids-free basis. This is despite the fact that it may be the properties of the suspensions proper that are important in many cases.

Surface tensions of aqueous solutions of inorganic electrolytes are well known to be larger than the surface tension of pure water at the same temperature. The surface tension of 2 M (10.5 mass%) sodium chloride solution is about 3.3 mN/m larger than the surface tension of

water at the same (room) temperature. It is commonly believed that the increased surface tension is due to strong interactions between water molecules and the ionic solutes. However, many other solutes cause the surface tensions of their solutions to be smaller than the surface tension of water at the same temperature.

Salmang et al. (*41*) and Taylor and Howlett (*42*) investigated physical properties of ceramic casting slips, which typically consist of suspensions of kaolinite in water in the presence of deflocculating agents. They found that the commonly used casting slip suspensions can have surface tensions that are several mN/m greater than that of pure water. Brian and Chen (*43*) measured the surface tensions of suspensions of iron oxide and silicon dioxide particles in two liquids (water and isoparaffin). Their surface tensions for suspensions of these solids in water were larger than for pure water, whereas suspensions in isoparaffin had surface tensions that were smaller than for the pure liquid. Schramm and Hepler (*44*) used two different methods to measure the surface tensions of aqueous suspensions of sodium montmorillonite and observed that these surface tensions are larger than those of pure water at the same temperatures (Figure 19). Figure 19 shows that dispersed montmorillonite also increases the suspension–toluene interfacial tension compared with that of pure water–toluene. Menon et al. (*45–47*) found that the presence of fine solids at an oil–water interface could either raise or lower interfacial tensions and explained their results in terms of different degrees of repulsive interaction among particles present at the interface. High interfacial coverages with charged shale dust particles were found to raise interfacial tension, but when the negative charge of the clays was
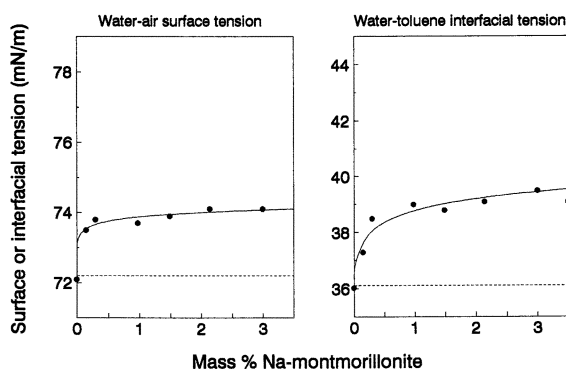
Figure 19.   Suspension–air and suspension–toluene surface and interfacial tensions for aqueous suspensions of Na-montmorillonite, as measured with the du Nouy ring technique at 24.5 °C. The broken lines show the values measured for pure water. (Reproduced with permission from reference 44. Copyright 1994 National Research Council of Canada.)

almost completely countered by the adsorption of asphaltenes, interfacial tension lowering was observed. Another feature of the particle interaction model is that dynamic surface or interfacial tensions might be expected because of the formation of a monolayer followed by particle rearrangements. Williams and Berg (48) support this finding and describe the phenomenon of adsorption and aggregation of colloidal particles at air–liquid interfaces.

It appears that aqueous suspensions of high charge density colloidal solids may exhibit raised surface and interfacial tensions compared with the corresponding solids-free systems and that the time dependence of suspension surface tensions can be appreciable. The effect of suspended particles of low charge density is much less clear. The effect of particle size on the surface or interfacial tensions of suspensions apparently has not been studied.

Contact Angles and Wetting.   Consider now what happens when a drop of oil in water comes into contact with a solid surface. The oil may form a bead on the surface or it may spread and form a film. A liquid having a strong affinity for the solid will seek to maximize its contact (interfacial area) and form a film. A liquid with much weaker affinity may form into a bead. The affinity is termed the wettability. Because there can be degrees of spreading, another quantity is needed. The contact angle, θ, in an oil–water–solid system is defined as the angle, measured through the aqueous phase, that is formed at the junction of the three phases. Whereas interfacial tension is defined for the boundary between two phases, the contact angle is defined for a three-phase junction.

If the interfacial forces acting along the perimeter of the drop are represented by the interfacial tensions, then an equilibrium force balance can be written as

$$\gamma_{W/O} \cos \theta = \gamma_{S/O} - \gamma_{S/W} \tag{24}$$

where the subscripts refer to water, W, oil, O, and solid, S. This is Young's equation. The solid is completely water wetted if $\theta = 0$ and only partially wetted otherwise. This equation is frequently used to describe wetting phenomena, so two practical points should be remembered. In theory, complete nonwetting by water would mean that $\theta = 180°$, but this is not seen in practice. Also, values of $\theta < 90°$ are often considered to represent "water-wetting," whereas values of $\theta > 90°$ are considered to represent "non-water-wetting." This is a rather arbitrary assignment based on correlation with visual appearance of drops on surfaces.

These considerations come into play in petroleum emulsions. The so-called Pickering emulsions are emulsions stabilized by a film of fine

particles. The most stable such emulsions occur when the contact angle is close to 90°, so that the particles will collect at the interface. One of the theories of emulsion type states that if an emulsifying agent is preferentially wetted by one of the phases, then more of the agent can be accommodated at the interface if that interface is convex toward that phase, that is, if that phase is the continuous phase. This works for both solids and surfactants as emulsifying agents (Bancroft's rule). Analogous to Bancroft's rule is that the liquid preferentially wetting the solid particles will tend to form the continuous phase. Thus, if there is a low contact angle ($\theta < 90°$ measured through the water phase), then an oil-in-water emulsion should form and a high contact angle ($\theta > 90°$) should produce a water-in-oil emulsion. Although there are many exceptions to such rules, they remain useful for making initial predictions.

In the earlier section on sedimentation, it was assumed that the particles were capable of sedimentation. But if dry particles are placed onto the surface of a body of liquid, they may not settle even though their density is greater than that of the liquid. The explanation provides an example of the actions of surface tension and contact angle. For a solid particle to float on a liquid surface, the upward pull of the meniscus around it (reflected in the surface tension and contact angle) must at least balance the weight of the particle. The surface tension and contact angle can be modified by adding species that alter the interfacial properties, for example, oils or surfactants. A needle can be made to float on water by coating it with oil so that the contact angle, θ, becomes $>90°$.

Consider a cube-shaped mineral particle having sides of length $L = 100$ μm and a density of 2.4 g/cm^3. If the particle is placed on the surface of a container of water of surface tension $\gamma = 72$ mN/m, it exhibits a contact angle of $\theta = 45°$ and a density difference $\Delta\rho = (2.4–1.0)$ g/cm^3. Ignoring the effects of immersion depth and taking upward force to be positive, the force due to surface tension is given by $-4L\gamma$ cos θ, whereas the force due to gravity is given by $-L^3 \Delta\rho g$. The net force is then approximately $-2.03 \times 10^{-2} - 1.37 \times 10^{-5}$ mN $= -2.03 \times 10^{-2}$ mN, the particle sinks.

This particle that does not naturally float can be made to float. Suppose that a surfactant is added to the water so that the solution surface tension becomes $\gamma = 40$ mN/m and the contact angle becomes $\theta = 140°$. In this case the net force on the particle becomes $+1.22 \times 10^{-2} - 1.37 \times 10^{-5}$ mN $= +1.22 \times 10^{-2}$ mN, the particle now floats.

Density and contact angle are usually modified in a froth flotation process. Thus, "collector" oils or surfactants can be added to ores that adsorb on desirable ore particles increasing the contact angle (and promoting attachment to gas bubbles) but that do not adsorb much on undesirable particles (which do not then attach to the gas bubbles). This

combined surface modification and gas bubble attachment allows the desired particles to be made lighter and selectively floated.

The simple example just presented forms the basis for a means of determining the hydrophobic index, an empirical measure of the relative wetting preference of very small solid particles. In one test method, solid particles of narrow size range are placed on the surfaces of a number of samples of water containing increasing concentrations of alcohol (thus providing a range of solvent surface tensions). The percentage alcohol solution at which the particles just begin to become hydrophilic and sink is taken as the hydrophobic index. The corresponding solvent surface-tension value is taken as the critical surface tension of wetting. The technique is also referred to as the film-flotation technique (49) or sink–float method.

List of Symbols

a	empirical viscosity constant (eq 8)
a	major particle dimension (eq 11)
a	particle radius (eqs 15, 17, 20–22)
A	Hamaker constant (eqs 17–19)
A_1	Hamaker constant for the medium (eq 18)
A_2	Hamaker constant for particles (eq 18)
A_{sp}	specific surface area (eq 23)
b	minor particle dimension (eq 11)
B	constant (eqs 15, 19)
c	concentration of particles (eq 3)
c_i	solution concentration of ions i
CCC	critical coagulation concentration (eq 19)
d	distance from a surface (same as x in eqs 12, 15, 17)
D	diffusion coefficient (eq 20)
e	charge on the electron (eqs 16, 19)
g	gravitational constant (eq 21)
H	distance from a surface (same as x in eqs 12, 15, 17)
I	ionic strength (eq 13)
I_d	intensity of light scattered by a particle in a suspension (eq 2)
I_0	intensity of incident light beam (eqs 1, 2)
I_t	intensity of transmitted light beam (eq 1)
k	Boltzmann's constant (eqs 15, 16, 19)
k_2	rate constant for aggregation
k_2^0	rate constant for diffusion controlled aggregation
K	Rayleigh constants (eq 3)
l	length of optical path through a sample (eq 1)
M	molar mass of particles (eq 3)
n	refractive index of a suspension (eq 3)

n	number of particles per unit volume at time t (eq 20)
n	number of spheres (eq 23)
n_0	refractive index of solvent (eq 3)
n_0	number of particles per unit volume at time $t = 0$ (eq 20)
N_A	Avogadro's number (eqs 3, 19)
r, R	particle radius (eqs 2, 23)
$R(\theta)$	Rayleigh ratio for a scattering angle of $\theta°$
R_{90}	Rayleigh ratio for a scattering angle of 90° (eq 3)
t	time (eqs 20–22)
T	absolute temperature (eqs 15, 16, 19)
V	total potential energy of interaction
V_A	attractive potential energy of interaction (eq 17)
V_R	repulsive potential energy of interaction (eq 15)
w	mass of particles falling the full length of a sedimentation column
W	in aggregation, stability ratio, $W = k_2^0/k_2$
W	in sedimentation, total mass of sedimenting particles
x	distance (eqs 2, 12, 15, 17, 21, 22)
z	counterion charge number (eqs 15, 16, 19)
z_i	charge number of ions i

Greek

γ	constant in repulsive potential energy equation (eqs 15, 16, 19)
γ	interfacial tension (eq 24)
$\dot{\gamma}$	shear rate (eqs 5, 6, 10)
$\gamma°$	surface tension
$\gamma_{S/O}$	solid–oil interfacial tension (eq 24)
$\gamma_{S/W}$	solid–water interfacial tension (eq 24)
$\gamma_{W/O}$	water–oil interfacial tension (eq 24)
ϵ	permittivity (eqs 15, 19)
ζ	zeta potential (eq 14)
η	viscosity (eqs 5–11, 21, 22)
η_0	viscosity of liquid continuous phase (eqs 7–11)
$[\eta]$	intrinsic viscosity (eq 10)
θ	contact angle (eq 24)
κ	conductivity of a dispersion (eq 4)
κ	$1/\kappa$ is the double layer thickness (eqs 12, 13, 15)
κ_D	conductivity of the dispersed phase (eq 4)
κ_C	conductivity of the continuous phase (eq 4)
λ	wavelength of light (eqs 2, 3)
μ_E	electrophoretic mobility

ρ	density (eq 23)
ρ_1	external fluid density (eqs 21, 22)
ρ_2	particle density (eqs 21, 22)
σ°	surface charge density
Σ_i	summation symbol
τ	turbidity (eq 1)
τ	shear stress (eq 5, 6)
τ_Y	yield stress (Figure 3)
ϕ	dispersed phase volume fraction (eqs 4, 7–11)
ψ°	surface electric potential (eq 12); ψ_0 in Figure 5)
ψ	electric potential at distance x from a surface (eq 12)
$\psi(\delta)$	electric potential at the Stern plane (eqs 14, 16)
ω	angular velocity (eq 22)

References

1. van Olphen, H. *An Introduction to Clay Colloid Chemistry*, 2nd ed.; Wiley-Interscience: New York, 1977.
2. Yariv, S.; Cross, H. *Geochemistry of Colloid Systems for Earth Scientists*; Springer-Verlag: Berlin, Germany, 1979.
3. *Dispersions of Powders in Liquids*, 2nd ed.; Parfitt, G. D., Ed; Applied Science Pub. Ltd.: London, 1973.
4. Shaw, D. J. *Introduction to Colloid and Surface Chemistry*, 3rd ed.; Butterworth: London, 1981.
5. Hiemenz, P. C. *Principles of Colloid and Surface Chemistry*, 2nd ed.; Marcel Dekker: New York, 1986.
6. Adamson, A. W. *Physical Chemistry of Surfaces*, 5th ed.; Wiley-Interscience: New York, 1990.
7. Ross, S.; Morrison, I. D. *Colloidal Systems and Interfaces*; Wiley: New York, 1988.
8. *Colloid Science*; Kruyt, H. R., Ed.; Elsevier: Amsterdam, Netherlands, 1952; Vol. 1.
9. Schramm, L. L. *The Language of Colloid and Interface Science*; American Chemical Society: Washington, DC, 1993.
10. Graham, T. *Philos. Trans.* **1861**, *151*, 183.
11. Laskowski, J. S.; Pugh, R. J. In *Colloid Chemistry in Mineral Processing*; Laskowski, J. S.; Ralston, J., Eds.; Elsevier: Amsterdam, Netherlands, 1992; pp 115–171.
12. Fallenius, K. *Acta Polytech. Scand.* **1977**, *138*, 1–30.
13. Becher, P. *Emulsions: Theory and Practice*, 2nd ed.; Krieger: Malabar, FL, 1977.
14. Williams, R. A.; Simons, S. J. R. In *Colloid and Surface Engineering*; Williams, R. A., Ed.; Butterworth-Heinemann: Oxford, U.K., 1992; pp 55–111.
15. Whorlow, R. W. *Rheological Techniques*; Wiley: New York, 1980.
16. Van Wazer, J. R.; Lyons, J. W.; Kim, K. Y.; Colwell, R. E. *Viscosity and Flow Measurement*; Wiley: New York, 1963.
17. Fredrickson, A. G. *Principles and Applications of Rheology*; Prentice-Hall: Englewood Cliffs, NJ, 1964.
18. Hunter, R. J. *Zeta Potential in Colloid Science*; Academic: Orlando, FL, 1981.

19. James, A. M. In *Surface and Colloid Science*; Good, R. J.; Stromberg, R. R., Eds.; Plenum: New York, 1979; Vol. 11, pp 121–186.
20. Riddick, T. M. *Control of Stability through Zeta Potential*; Zeta Meter, Inc.: Staunton, VA, 1968.
21. O'Brien, R. W.; White, L. R. *J. Chem. Soc. Faraday Trans. 2* **1978,** *74,* 1607–1626.
22. Overbeek, J. Th. G. In *Colloidal Dispersions*; Goodwin, J. W., Ed.; Special Publication 43; Royal Society of Chemistry: London, 1982; pp 1–21.
23. Derjaguin, B. V.; Churaev, N. V.; Miller, V. M. *Surface Forces*; Consultants Bureau: New York, 1987.
24. Verwey, E. J. W.; Overbeek, J. Th. G. *Theory of the Stability of Lyophobic Colloids*; Elsevier: New York, 1948.
25. Luckham, P. F.; de Costello, B. A. *Adv. Colloid Interface Sci.* **1993,** *44,* 183–240.
26. Williams, R. A.; Jia, X. *Chem. Ind. (London)* **1992,** *11,* 409–412.
27. Grim, R. E. *Clay Mineralogy*, 2nd ed.; McGraw-Hill: New York, 1968.
28. Schramm, L. L.; Kwak, J. C. T. *Clays Clay Miner.* **1982,** *30,* 40–48.
29. Schramm, L. L.; Kwak, J. C. T. *Colloids Surf.* **1982,** *3,* 43–60.
30. Alince, B.; Van de Ven, T. G. M. *J. Colloid Interface Sci.* **1993,** *155,* 465–470.
31. Gregory, J. *Crit. Rev. Environ. Control* **1989,** *19,* 185–230.
32. Russel, W. B.; Saville, D. A.; Schowalter, W. R. *Colloidal Dispersions*; Cambridge University: Cambridge, U.K., 1991.
33. Overbeek, J. Th. G. In *Colloid Science*; Kruyt, H. R., Ed.; Elsevier: Amsterdam, Netherlands, 1952; Vol. 1, pp 194–244.
34. Morrison, I. D. *Colloids Surf. A* **1993,** *71,* 1–37.
35. Shaw, R. C.; Czarnecki, J.; Schramm, L. L.; Axelson, D. In *Foams: Fundamentals and Applications in the Petroleum Industry*; Schramm, L. L., Ed.; ACS Advances in Chemistry 242; American Chemical Society: Washington, DC, 1994; pp 423–459.
36. Schramm, L. L.; Kwak, J. C. T. *J. Can. Petrol. Technol.* **1988,** *27,* 26–35.
37. Schramm, L. L. In *Emulsions: Fundamentals and Applications in the Petroleum Industry*; Schramm, L. L., Ed.; ACS Advances in Chemistry 231; American Chemical Society: Washington, DC, 1992; pp 1–49.
38. Harkins, W. D.; Alexander, A. E. In *Physical Methods of Organic Chemistry*; Weissberger, A., Ed.; Interscience: New York, 1959; pp 757–814.
39. Padday, J. F. In *Surface and Colloid Science*; Matijevic, E., Ed.; Wiley-Interscience: New York, 1969; Vol. 1, pp 101–149.
40. Miller, C. A.; Neogi, P. *Interfacial Phenomena Equilibrium and Dynamic Effects*; Marcel Dekker: New York, 1985.
41. Salmang, H.; Deen, W.; Vroemen, A. *Ber. Dsch. Keram. Ges.* **1957,** *34,* 33–38.
42. Taylor, D.; Howlett, D. J. *Trans. J. Brit. Ceram. Soc.* **1974,** *73,* 19–22.
43. Brian, B. W.; Chen, J. C. *AIChE J.* **1987,** *33,* 316–318.
44. Schramm, L. L.; Hepler, L. G. *Can. J. Chem.* **1994,** *72,* 1915–1920.
45. Menon, V. B.; Nikolov, A. D.; Wasan, D. T. *J. Colloid Interface Sci.* **1988,** *124,* 317–327.
46. Menon, V. B.; Nikolov, A. D.; Wasan, D. T. *J. Dispersion Sci. Technol.* **1988/89,** *9,* 575–593.
47. Menon, V. B.; Wasan, D. T. *Colloids Surf.* **1988,** *29,* 7–27.
48. Williams, D. F.; Berg, J. C. *J. Colloid Interface Sci.* **1992,** *152,* 218–229.
49. Fuerstenau, D. W.; Williams, M. C. *Colloids Surf.* **1987,** *22,* 87–91.

50. *Zeta-Meter Applications Brochures;* Zeta-Meter, Inc.: Staunton, VA, 1982.
51. Schramm, L. L. Ph.D. Thesis, Dalhousie University, Halifax, Canada, 1980.
52. Mysels, K. J. *Introduction to Colloid Chemistry;* Interscience: New York, 1959.
53. Barnes, H. A.; Holbrook, S. A. In *Processing of Solid–Liquid Suspensions;* Ayazi Shamlou, P., Ed.; Butterworth-Heinemann: Oxford, U.K., 1993; pp 222–245.
54. Lake, L. W. *Enhanced Oil Recovery;* Prentice Hall: Englewood Cliffs, NJ, 1989; pp. 47–48.
55. Clark, R. K.; Nahm, J. J. In *Kirk–Othmer Encyclopedia of Chemical Technology,* 3rd ed.; Wiley: New York, 1982; Vol. 17, pp 143–167.